

Figure S1: Loss of function of beta-catenin results in an anteriorization of the hypothalamus. A-U: *In situ* hybridization of hypothalamic markers on E12.5 control (*Cre*-negative, either *Ctnnb1*^{lox/lox} or *Ctnnb1*^{lox/+}) and *Nkx2.1-Cre;Ctnnb1*^{lox/lox} coronal sections. A-J: The mamillary was reduced (black arrowheads) but the PVN was unaffected (open arrowheads). K-U: The hypothalamic neuroepithelium was thinned in the mutant (black arrowheads), while the pituitary was misplaced (open arrowheads).

Figure S2: Loss of function of beta-catenin results in an anteriorization of the hypothalamus. A-B': *In situ* hybridization of hypothalamic markers on E12.5 control (*Cre*-negative, either *Ctnnb1*^{lox/lox} or *Ctnnb1*^{lox/+}) and *Nkx2.1-Cre;Ctnnb1*^{lox/lox} coronal sections. A-H: The TT (open arrowheads) was lost and ID (black arrowheads) ventralized in the mutant. I-B': Anterior structures were expanded posteriorly in the mutants. I-R: black arrowheads indicate the arcuate. S-B': black arrowheads indicate the VMH.

Figure S3: Loss of function of beta-catenin results in a thinning and anteriorization of the hypothalamus, but has no effect on prethalamus. *In situ* hybridization on E12.5 control (*Cre*-negative, either *Ctnnb1*^{lox/lox} or *Ctnnb1*^{lox/+}) and *Foxd1-Cre;Ctnnb1*^{lox/lox} coronal sections. A-L: The hypothalamic domains were reduced (open arrowheads), but the prethalamic domains were unaffected (black arrowheads). M-R: Precursors of orexinergic hypocretin neurons (marked here by *Lhx9* expression) were normal, but ventralized due to the thinned hypothalamus (black arrowheads). S-X: The arcuate (black arrowheads) was displaced due to the invasion of the pituitary.

Figure S4: Constitutively active beta-catenin results in disrupted patterning and development of the hypothalamus and prethalamus. A-X: *In situ* hybridization on E12.5 control (*Foxd1-Cre*-negative;*Ctnnb1*^{ex3/+}) and *Foxd1-Cre;Ctnnb1*^{ex3/+} coronal sections. A-L: The prethalamic (black arrowheads) and hypothalamic (open arrowheads) expression domains were reduced. G-L: M-R: *Lhx1* expression in the ZLI (black arrowheads), prethalamus (open arrowheads), ID (red arrowheads), anterior hypothalamus (yellow arrowhead) and mamillary (green arrowheads) was lost everywhere except the ZLI and mamillary, where signal was reduced. S-X: *Pitx2* in the supramamillary/mamillary region (open arrowheads) was expanded.

Figure S5: Constitutively active beta-catenin results in disrupted patterning and development of the hypothalamus. A-X: *In situ* hybridization on E12.5 control (*Foxd1-Cre*-negative;*Ctnnb1*^{ex3/+}) and *Foxd1-Cre;Ctnnb1*^{ex3/+} coronal sections. A-L: *Lhx9* in the orexinergic neurons (black arrowheads, A-F), and *Ntng2* in the premamillary (open arrowheads, G-L) were both expanded. M-R: The premamillary domain of *Bsx* was present (black arrowheads) but the arcuate expression was lost (open arrowheads) in the GOF mutant. There was ectopic expression in the developing habenula (red arrowhead). The ZLI was

unaffected (black arrowheads, G-R). S-X: *Lhx6* was lost in the ID (open arrowhead) and TT (black arrowheads).

Figure S6: Constitutively active beta-catenin results in disrupted patterning and development of the hypothalamus. Constitutively active β -catenin results in a disrupted and expanded arcuate (A-F) and ventral hypothalamus (G-L) and mosaic expression of *Pomc* (black arrowheads, A-F) and *Rax* (black arrowheads, G-L). I: Open arrowhead indicates the infundibulum.

Figure S7: Loss of function of beta-catenin had no effect on proliferation, but constitutively active beta-catenin increased proliferation. A-C: EdU and DAPI staining after a 2hr EdU pulse in coronal E12.5 sections from *Foxd1*-Cre-negative; *Ctnnb1*^{lox/lox}, *Foxd1*-Cre;*Ctnnb1*^{lox/lox} and *Foxd1*-Cre;*Ctnnb1*^{ex3/+} embryos. Red scroll bars indicate the boundary of the prethalamus and hypothalamus. D: Quantification of EdU counts relative to area in control versus β -catenin LOF brains (n=3).

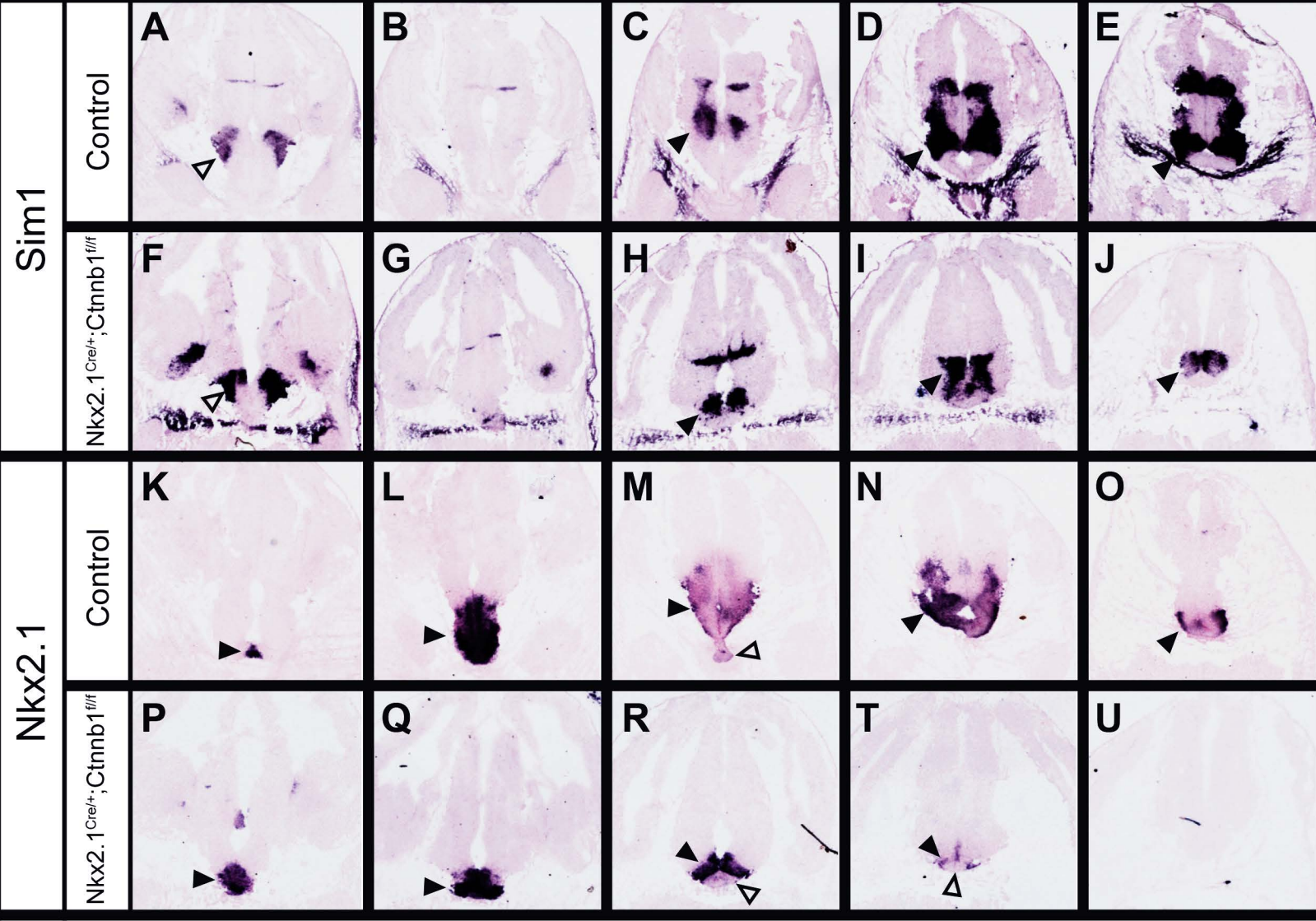


Figure S1, Newman et al.

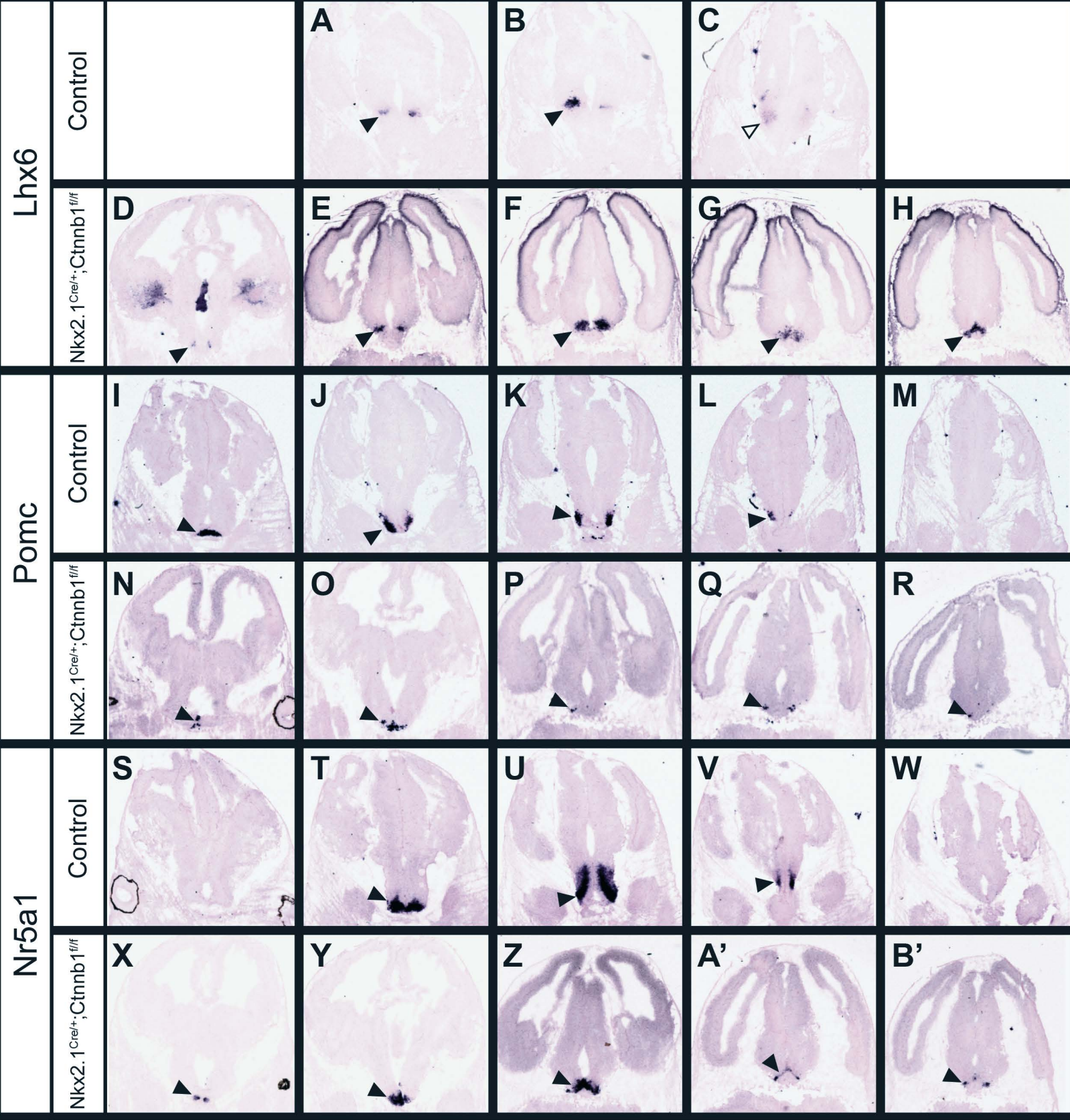


Figure S2, Newman et al.

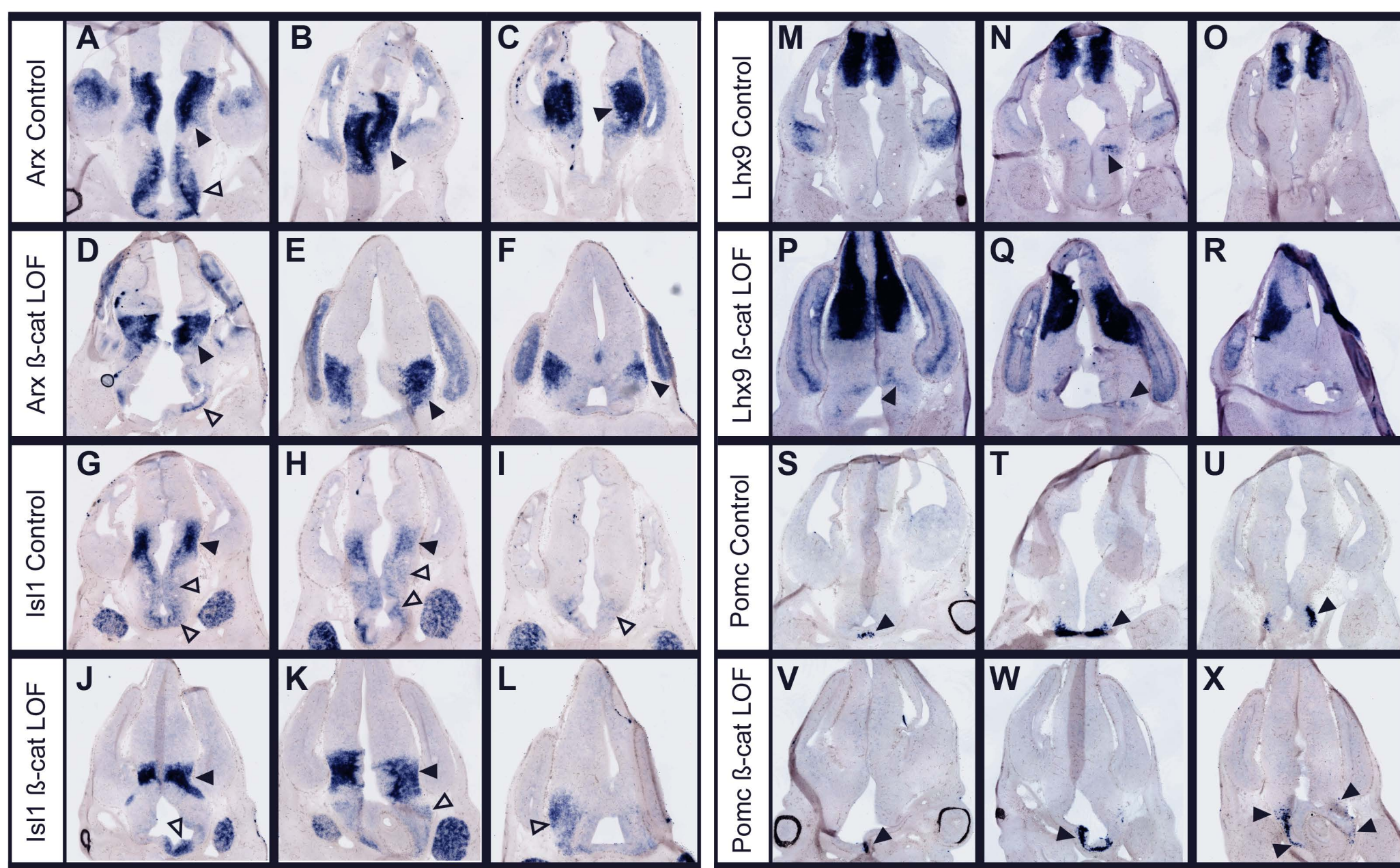


Figure S3, Newman et al.

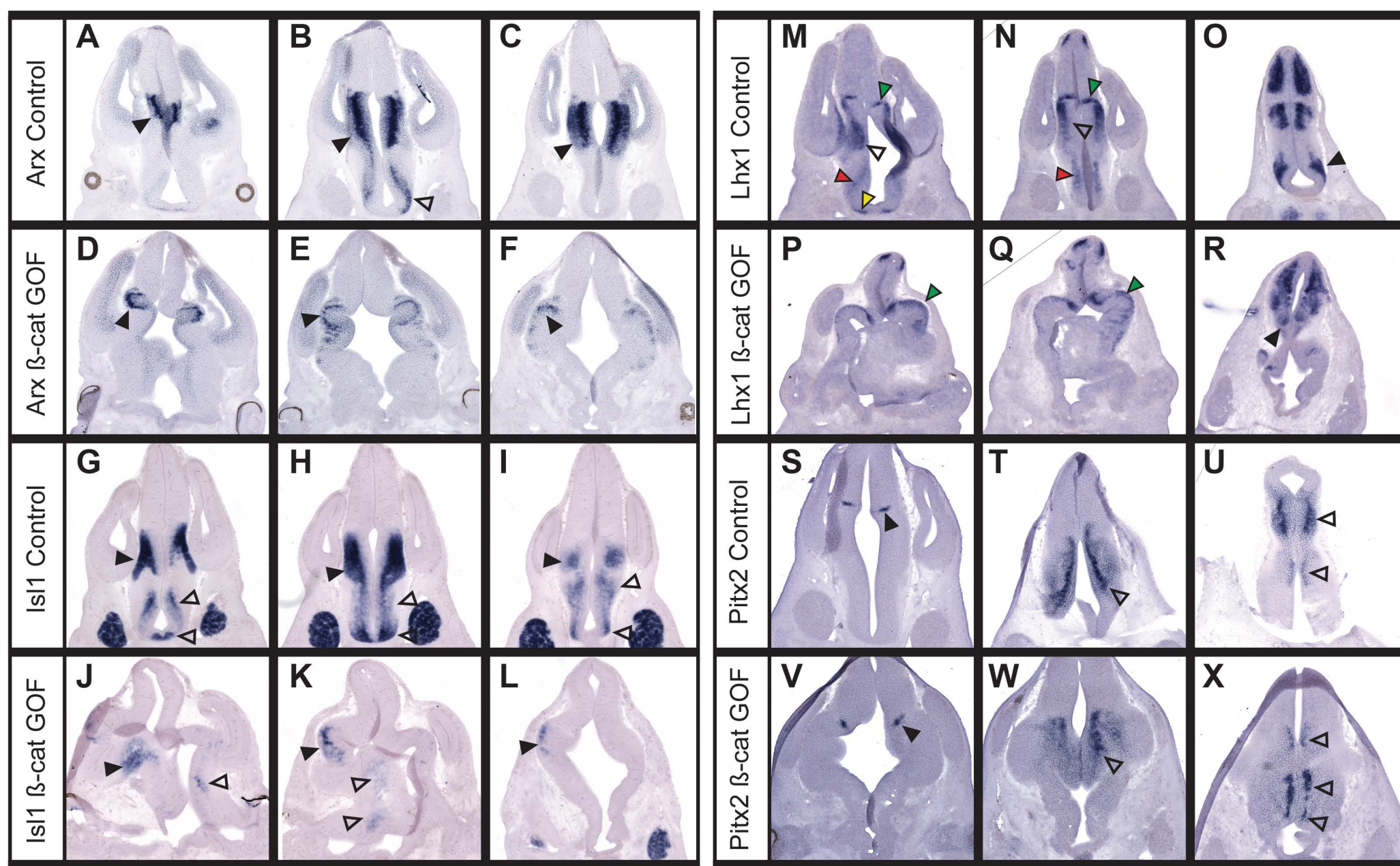


Figure S4, Newman et al.

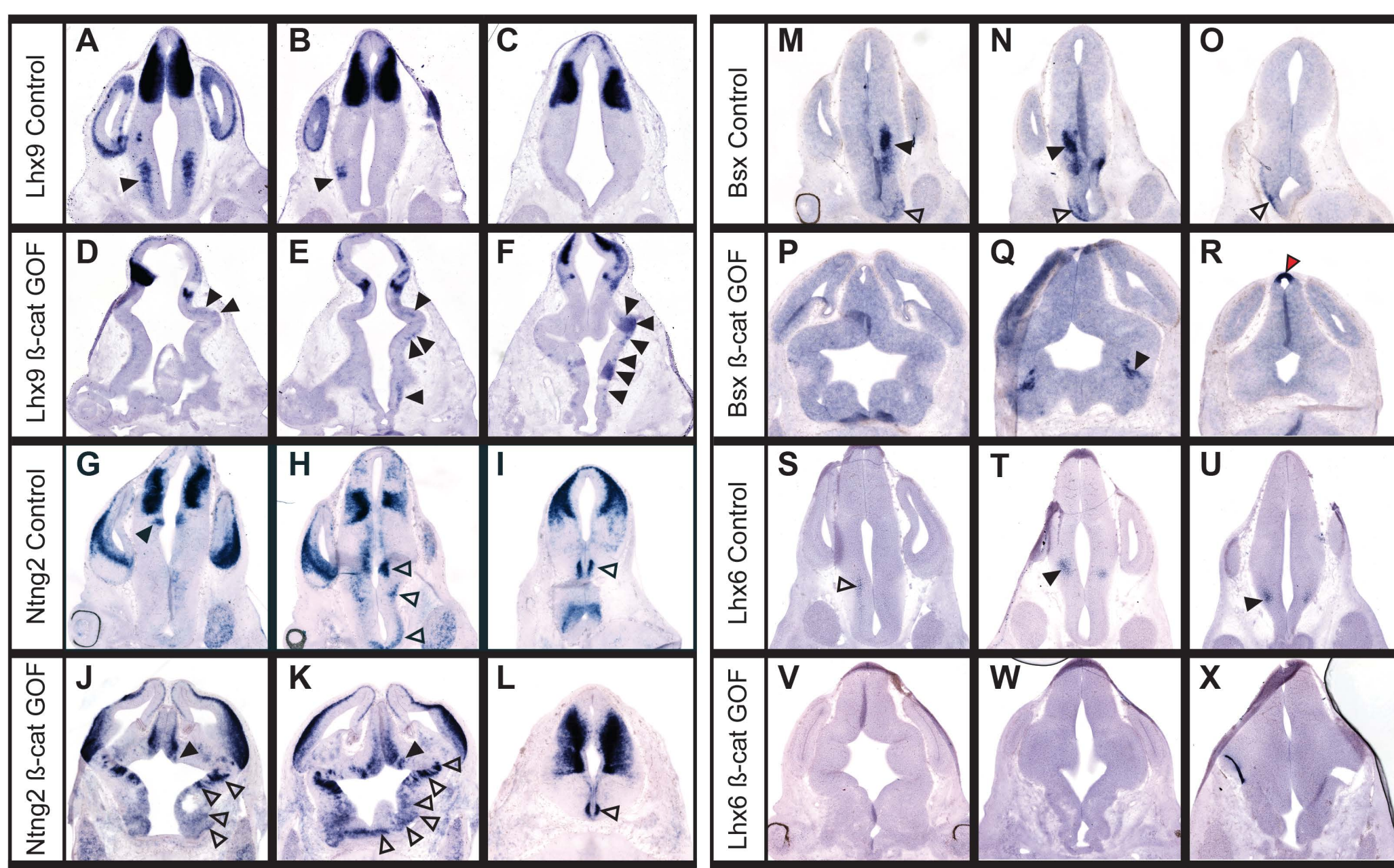


Figure S5, Newman et al.

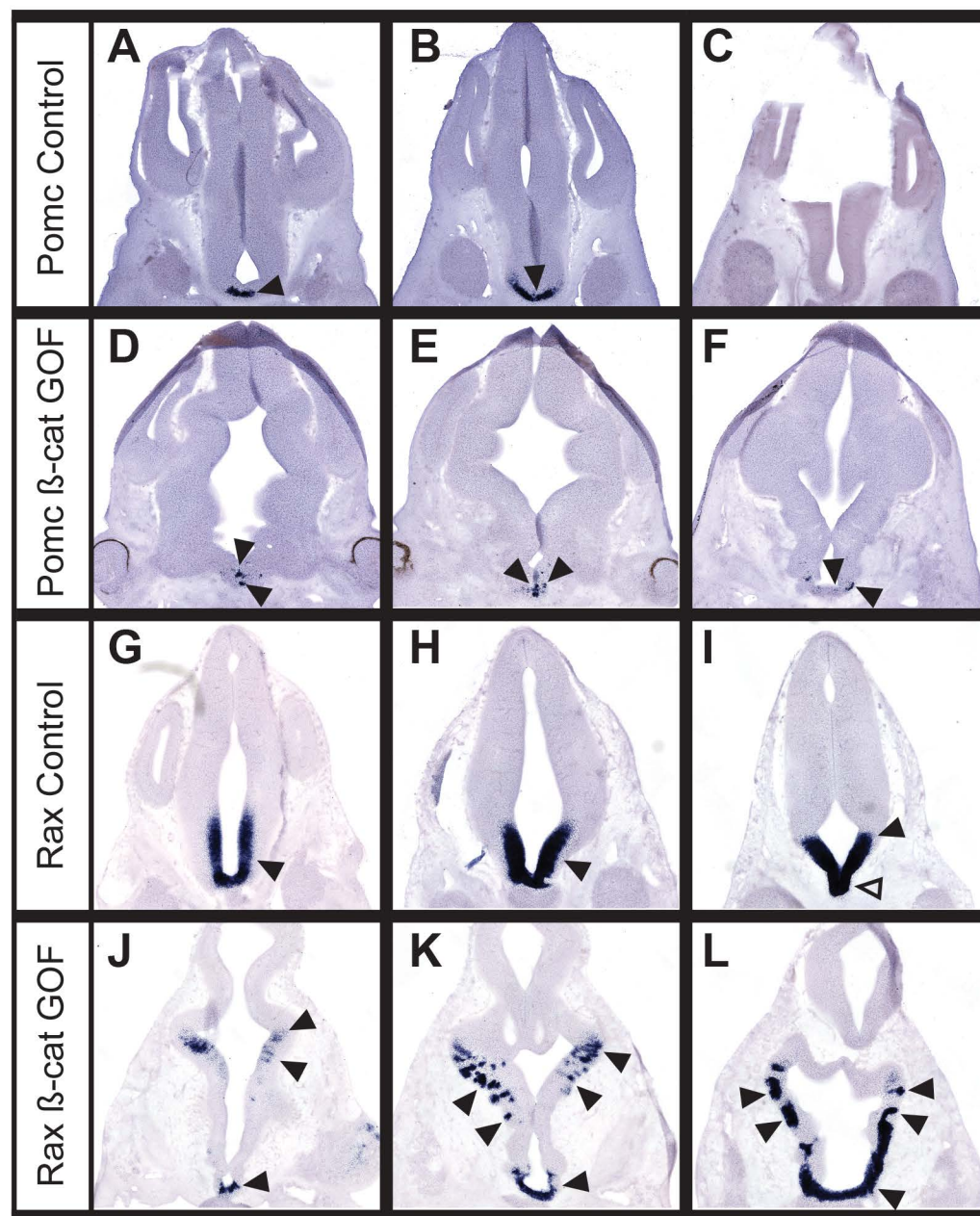


Figure S6, Newman et al.

